Inhibition of HIV-1 Reverse Transcriptase-Catalyzed DNA Strand Transfer Reactions by 4-Chlorophenylhydrazone of Mesoxalic Acid[†]

Wendolyn R. Davis, John Tomsho, Savita Nikam, Elizabeth M. Cook, David Somand, and James A. Peliska*

Department of Biological Chemistry, University of Michigan Medical School, Ann Arbor, Michigan 48109-0606

Received July 7, 2000; Revised Manuscript Received September 13, 2000

ABSTRACT: DNA strand transfer reactions occur twice during retroviral reverse transcription catalyzed by HIV-1 reverse transcriptase. The 4-chlorophenylhydrazone of mesoxalic acid (CPHM) was found to be an inhibitor of DNA strand transfer reactions catalyzed by HIV-1 reverse transcriptase. Using a model strand transfer assay system described previously [Davis, W. R., et al. (1998) *Biochemistry 37*, 14213−14221], the mechanism of CPHM inhibition of DNA strand transfer has been characterized. CPHM was found to target the RNase H activity of HIV-1 reverse transcriptase. DNA polymerase activity was not significantly affected by CPHM; however, it did inhibit the polymerase-independent RNase H activity with an IC_{50} of 2.2 μM. In the absence of DNA synthesis, CPHM appears to interfere with the translocation, or repositioning, of RT on the RNA·DNA template duplex, a step required for efficient RNA hydrolysis by RNase H. Enzyme inhibition by CPHM was found to be highly specific for HIV-1 reverse transcriptase; little or no inhibition of DNA strand transfer or DNA polymerase activity was observed with MLV or AMV reverse transcriptase, T7 DNA polymerase, or DNA polymerase I. Examination of additional 4-chlorophenylhydrazones showed that the dicarboxylic acid moiety of CPHM is essential for activity, suggesting its important role for enzyme binding. Consistent with the role of the dicarboxylic acid in inhibitor function, Mg^{2+} was found to chelate directly to CPHM with a K_d of 2.4 mM. Together, these studies suggest that the inhibitor may function by binding to enzyme-bound divalent metal cofactors.

The enzyme HIV-1 reverse transcriptase (RT)[1] catalyzes a complex series of reactions during the process of reverse transcription. To accomplish this process, RT utilizes two catalytic active sites located on the same protein. HIV-1 RT, a heterodimeric protein consisting of 66 and 51 kDa subunits, displays three catalytic activities: RNA-dependent DNA polymerization, wherein DNA is synthesized using an RNA template; DNA-dependent DNA polymerization, where DNA serves as a template; and an RNase H activity, which catalyzes the selective hydrolysis of RNA from DNA·RNA heteroduplexes (*1*, *2*). The RNase H activity of RT has been classified as having two kinetically distinguishable activities termed polymerase-dependent (*3*, *4*) and polymerase-independent (*5*). Polymerase-dependent RNase H activity cleaves RNA from RNA·DNA heteroduplexes concomitant with DNA polymerization, while the term polymerase-independent activity describes RNase H hydrolysis in the absence of DNA polymerization. The polymerase-dependent RNase H cleavages are concomitant with DNA elongation, with 18−19 nucleotide base pairs between the primer terminus and cleavage site. This pattern represents the distance between the polymerase and RNase H active sites of HIV-1 RT (*4*, *6*−*8*). During this mode of enzyme action, the template·primer complex is positioned such that its 3′-terminus is situated in the DNA polymerase active site and the DNA·RNA template·primer complex spans the polymerase and RNase H domains. Alternatively, during polymerase-independent RNase H activity, the template·primer complex can bind with alternate positioning where the 3′-terminus of the primer is no longer restrained to the polymerase active site, giving rise to alternate RNase H cleavage sites not occurring during DNA polymerizaton.

Both in vitro model and viral systems show that the RNase H functions of HIV-1 RT are essential for catalyzing DNA strand transfer events during reverse transcription (*5*, *9*−*13*). DNA strand transfer is a process by which a newly synthesized DNA is physically translocated from one RNA or DNA "donor" template to a second RNA or DNA "acceptor" template. Two strand transfer events are obligatory for the production of double-stranded proviral DNA during the reverse transcription process (*14*). However, due to the homologous nature of the diploid RNA genome, strand transfer can occur at internal regions of the genome as well, leading to recombinant proviral products (*15*).

Kinetic studies using in vitro model systems have begun to characterize intermediates of the DNA strand transfer process. Still, further mechanistic characterization is hindered due to the complexity of the strand transfer reaction. One

[†] This work was funded in part by Pharmacological Sciences Training Grant GM 07767 from NIGMS (W.R.D. and J.T.) and NIH Grant AI42844 (J.A.P.).

* To whom correspondence should be addressed: Department of Biological Chemistry, University of Michigan Medical Center, 1301 E. Catherine, Ann Arbor, MI 48109-0606. Phone: (734) 763-8067. Fax: (734) 763-4581. E-mail: peliska@umich.edu.

[1] Abbreviations: HIV-1, human immunodeficiency virus type 1; AIDS, acquired immunodeficiency syndrome; RNase H, ribonuclease H; NC, nucleocapsid protein; RT, reverse transcriptase; EDTA, ethylenediaminetetraacetic acid; TBE, Tris/boric acid/EDTA buffer; DTT, dithiothreitol; Tris, tris(hydroxymethyl)aminomethane; IPTG, isopropyl β-D-thiogalactopyranoside; DMSO, dimethyl sulfoxide; PAGE, polyacrylamide gel electrophoresis.

10.1021/bi0015764 CCC: $19.00
Published on Web 10/24/2000

model for DNA strand transfer proposes that after RT pauses, either by reaching the end of its template or due to polymerase stalling, the enzyme dissociates from the complex and in conjunction with RNase H-catalyzed hydrolysis initiates nascent DNA transfer onto an acceptor template (*16*). An alternative model proposes that RT helps facilitate strand transfer via higher-order nucleic acid−protein intermediates (*5*, *17*). Other studies strongly suggest that other viral proteins are involved in the process of strand transfer. HIV-1 nucleocapsid protein (NC) is present at high concentrations in the virion particle and has been shown to accelerate DNA strand transfer in vitro (*12*, *18*−*22*), suggesting that strand transfer occurs in a complex of proteins, including NC (*19*, *20*, *23*−*28*).

Because of the key role of RT in retroviral replication, it has been a primary target for the identification and development of inhibitors that are suitable for the therapeutic treatment of HIV-1 infections. These RT inhibitors generally fall into two classes (*29*). Nucleoside analogues are represented by compounds such as 3′-azido-3′-deoxythymidine (AZT), 2′,3′-dideoxyinosine (ddI), 2′,3′-dideoxycytidine (ddC), (−)-2′-deoxy-3′-thiacytidine (3TC), 2′,3′-didehydro-2′,3′-dideoxythymidine (d4T), and (−)-2′,3′-dideoxy-5-fluoro-3′-thiacytidine (FTC) (*30*). While these inhibitors bind competitively with dNTPs at the polymerase active site, their antiviral activities stem from their ability to act as DNA synthesis chain terminators. A second class of inhibitors, termed nonnucleoside RT inhibitors, includes tetrahydroimidazobenzodiazepinone (TIBO), hydroxyethoxymethylphenlthiothymine (HEPT), dipyridodiazepinone (nevirapine), and bis(heteroaryl)piperazine (BHAP) (*31*). TIBO and nevirapine have been shown to bind RT in a hydrophobic region of the p66 subunit of RT close to the polymerase active site (*8*, *32*, *33*). Pre-steady-state burst studies of RT-catalyzed DNA polymerization in the presence of TIBO demonstrated that it blocked the chemistry step of nucleotide incorporation without interfering with nucleotide binding (*34*). While nevirapine has been shown to bind at a site distant from the RNase H active site (*8*), there is evidence showing that it can affect the RNase H activity of HIV-1 RT (*35*). This suggests that nevirapine has multiple effects on HIV-1 RT (*35*, *36*). Both classes of RT inhibitors are limited by their cellular toxicity and the emergence of drug resistant virus (*37*).

While the RNase H activity of HIV-1 RT is mandatory for viral replication, surprisingly few inhibitors of RNase H function have been identified. Several modes of RNase H inhibition can be conceived: (1) disruption or blocking of RNA−DNA binding to the enzyme active site, (2) attenuation of RNase H catalytic activity, and (3) interfering with important interactions between the polymerase and RNase H domains (*38*). Known inhibitors of HIV-1 RT RNase H include cysteine-modifying reagents (*39*), naphthalenesulfonic acid analogues (*40*), the natural marine product illimaquinone (*41*−*43*), and the metal chelator, *N*-(4-*tert*-butylbenzoyl)-2-hydroxy-1-naphthaldehyde hydrazone (BBNH) (*44*). However, the potency of these compounds is variable, and they generally inhibit both the DNA polymerase and RNase H activities of HIV-1 RT.

We have reported the identification of novel inhibitors of DNA strand transfer reactions catalyzed by HIV-1 reverse transcriptase (*45*) and the mechanistic characterization of one of these inhibitors, actinomycin D (*46*−*48*). This report focuses on the kinetic and mechanistic characterization of a second inhibitor of DNA strand transfer, the 4-chlorophenylhydrazone of mesoxalic acid (CPHM). We have demonstrated that this compound inhibits DNA strand transfer reactions by specifically targeting the DNA polymerase-independent RNase H activity of HIV-1. Furthermore, CPHM was found to be specific for HIV-1 reverse transcriptase, showing no inhibition in assays in which DNA polymerase and RNaseH activities of other reverse transcriptases and DNA polymerases are examined. The dicarboxylic acid moiety of CPHM is implicated in binding the divalent metal cofactor, and it is shown that this inhibitor directly chelates Mg^{2+} under the conditions used in enzyme activity assays. Together, these studies identify possible new mechanistic approaches for inhibiting HIV-1 RT function.

MATERIALS AND METHODS

Materials. HIV-1 RT was purified as described previously (*46*). The sequences of oligonucleotides used in the strand transfer, RNase hydrolysis, and extension assays are shown in Figure 1. The methods for synthesis and purification of oligonucleotides have been described previously (*46*).

All buffers were prepared from the highest-quality RNase-free reagents. CPHM was obtained from Parke-Davis pharmaceuticals. T_4 polynucleotide kinase was obtained from New England BioLabs. *Escherichia coli* RNase HI, AMV reverse transcriptase, and M-MLV reverse transcriptase were obtained from Gibco/Life Technologies. All other reagents were of the highest quality commercially available.

The ^{1}H NMR and mass spectroscopy analysis of all synthetic compounds were consistent with the structures shown in Scheme 1. UV−visible spectroscopy was performed using a Shimadzu UV-2501 PC spectrophotometer.

Synthesis of 4-Chlorophenylhydrazone of Pyruvic Acid (Scheme 1). Pyruvic acid sodium salt (0.22 g, 2 mmol) was added to a solution of 5 mL of dH_2O and 0.5 mL of glacial acetic acid with stirring until a clear solution formed. 4-Chlorophenylhydrazine hydrochloride (0.36 g, 2 mmol) was then added, and the solution was stirred for 10 min. The reaction mixture was then extracted with 3 × 15 mL of ethyl acetate, and the combined organic layers were washed with 10 mL of brine. The organic layer was dried over anhydrous magnesium sulfate, and another 0.5 mL of glacial acetic acid was added. The compound was heated to reflux, cooled to room temperature, and filtered. The residual glacial acetic acid was removed by repeated addition and rotary evaporation of ethyl acetate. The solid was resuspended in dichloromethane and filtered to yield 0.34 g (81% yield) of the pyruvic acid 4-chlorophenylhydrazone: mp 195−196 °C dec; TLC (EtOAc/HOAc) $R_f = 0.70$.

Synthesis of 4-Chlorophenylhydrazone of Acetone (Scheme 1). 4-Chlorophenylhydrazine hydrochloride (0.36 g, 2 mmol) was dissolved in a solution of 5 mL of 100% ethanol (ketone and aldehyde free), 4.5 mL (∼80 mmol) of acetone, and 0.5 mL of glacial acetic acid. The mixture was stirred for 15 min at room temperature, and the solvents were removed by rotary evaporation. The residue was diluted with 100% ethanol/acetone (1/1) and concentrated repeatedly to remove acetic acid. Residual solvents were removed in vacuo. The resulting residue was resuspended with acetone, and the solid

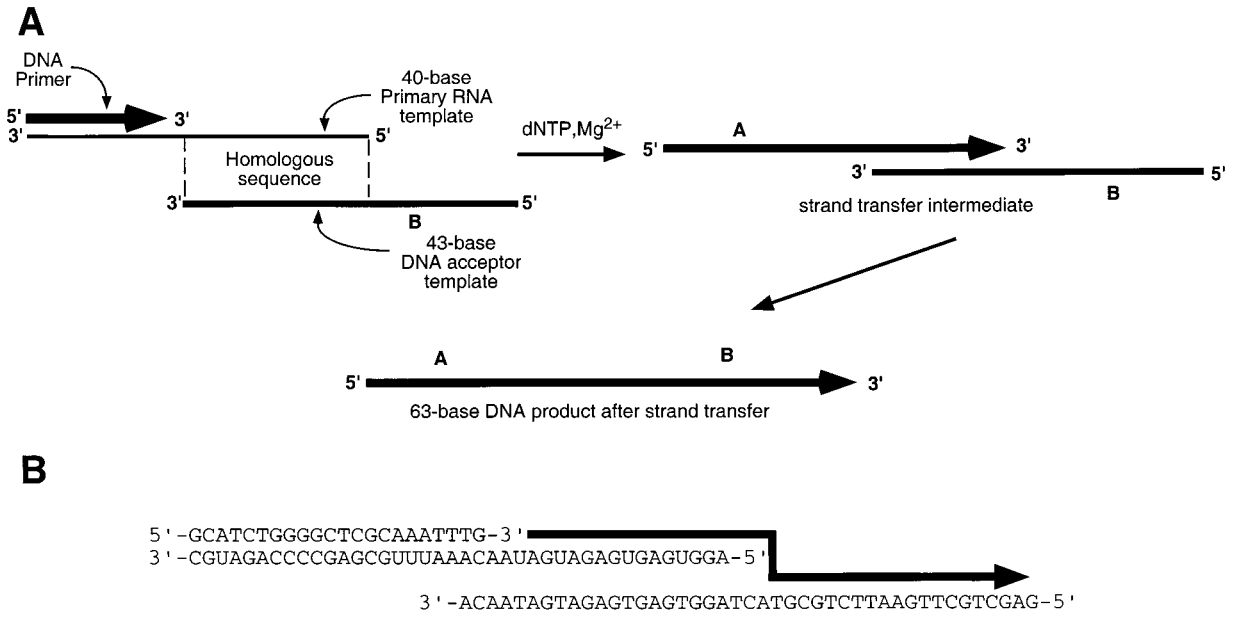

FIGURE 1: DNA strand transfer assay system. (A) A template·primer system consisting of a 22-base primer annealed to a 40-base primary RNA template was used in the presence of a 43-base DNA acceptor that is homologous to the 20 bases at the 5′-end of the primary RNA template, and containing an additional 23 bases. The DNA primer was radioactively labeled at its 5′-end, annealed to the template RNA, and preincubated in the presence of HIV-1 RT and other necessary components as described in Materials and Methods. Reactions were initiated with dNTPs and $MgCl_2$, aliquots withdrawn, reactions quenched in EDTA, and mixtures analyzed with denaturing PAGE. DNA strand transfer is indicated by the production of a 63-base DNA product. (B) Sequences of DNA and RNA substrates used in DNA strand transfer reactions. The arrow shows the direction of DNA synthesis during strand transfer.

Scheme 1

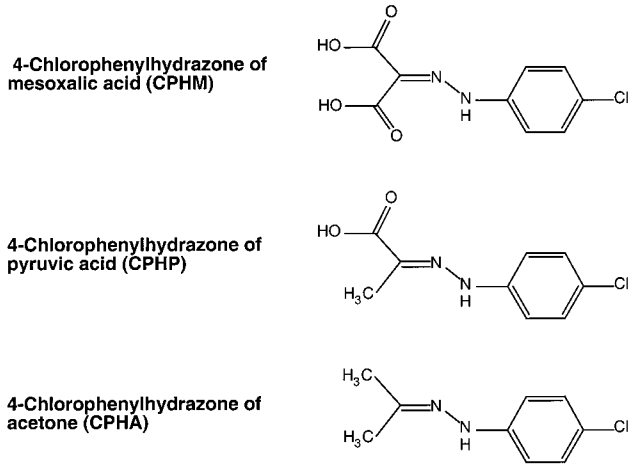

was filtered off, yielding 0.29 g (81% yield) of acetone 4-chlorophenylhydrazone: mp 123−125 °C dec; TLC (EtOH/Et_3N) $R_f = 0.87$.

DNA Strand Transfer and HIV-1 RT RNase H Assays. DNA strand transfer reactions and HIV-1 RT RNase H assays were performed with slight modifications as previously described (*46*). Briefly, a reaction mixture containing reaction buffer [63 mM Tris-HCl (pH 7.6), 60 mM KCl, and 1 mM EDTA (pH 8)], 20 nM 22-base DNA primer·40-base RNA template duplex (^{32}P-5′-end labeled on either the DNA or RNA), 400 nM DNA acceptor template, 20 nM HIV-1 RT, and varying amounts of CPHM in DMSO were preincubated at 37 °C for 5 min. Reactions were initiated with 10 mM $MgCl_2$/0.1 mM dNTPs, and samples were withdrawn and the reactions quenched into 50 mM EDTA/denaturing load buffer. Samples were resolved on 20% denaturing polyacrylamide gels, and products were visualized and quantitated with a Molecular Dynamics PhosphorImager and quantitated with Imagequant 1.1 software. The effect of CPHM on steady-state RNase H was tested as in the RNase H assay described above except that the template·primer complex was held at a 10-fold excess of RT in the reaction. Inhibition of CPHM on *E. coli* RNase H was performed as described above except that $MgCl_2$ alone was used to initiate reactions.

DNA·DNA template·primer extension experiments were performed as described for the strand transfer experiments except that a DNA·DNA template·primer complex consisting of the ^{32}P-5′-labeled 40-base primary DNA product·43-base acceptor template was used instead of the 22-base DNA primer·40-base RNA template system.

Effect of CPHM on Pre-Steady-State Kinetics of dTTP Incorporation and RNA Hydrolysis. A reaction mixture containing reaction buffer [63 mM Tris-HCl (pH 7.6) and 60 mM KCl], 20 nM doubly labeled ^{32}P-5′-labeled 40-base RNA template·^{32}P-5′-labeled 22-base DNA primer (*36*, *49*), 30 nM HIV-1 RT, and either 0 or 75 μM CPHM in DMSO was incubated on ice for 5 min. The mixture was then loaded into a Kin-Tek model RQF-3 quench-flow apparatus which had been pre-equilibrated to 37 °C. Reactions were initiated with 10 mM $MgCl_2$ and 0.1 mM dTTP at the indicated time points and then quenched with 0.5 M EDTA. All concentrations that are listed are final concentrations unless otherwise specified. The zero point represents a prequenched reaction. Samples were diluted into denaturing load buffer and resolved by denaturing PAGE (20% acylamide/8 M urea/TBE). Bands were visualized using a Molecular Dynamics Phosphorimager and quantitated with Imagequant version 1.1 software. Pre-steady-state burst rates and amplitudes were determined as described previously (*49*).

Specificity Studies of the Inhibition of Reverse Transcriptase and DNA Polymerase Activities. The ability of

CPHM to inhibit DNA strand transfer of other reverse transcriptases was performed using reactions similar to those described above. A reaction mixture containing reaction buffer, 20 nM ^{32}P-5′-labeled 22-base DNA primer·40-base RNA template, 400 nM DNA acceptor template, 10 units of reverse transcriptase (AMV or M-MLV), and various amounts of inhibitor CPHM (0−100 μM) was incubated at 37 °C for 5 min. Reactions were initiated by the addition of dNTP (0.1 mM each) and 10 mM $MgCl_2$ (final concentration). Reaction samples were withdrawn at different times and reactions quenched into 10 mM EDTA/denaturing load buffer. Samples were resolved by denaturing PAGE (20% acrylamide/8 M urea/TBE). Product bands were visualized using a Phosphorimager and quantitated using Imagequant version 1.1 software.

A similar reaction was used to examine DNA polymerase extension activity inhibition of DNA polymerase I Klenow fragment and T4 DNA polymerase. Instead of a DNA·RNA primer·template complex as for DNA strand transfer, the reaction mixture contained a template primer composed of ^{32}P-5′-labeled 20-base DNA primer·33-base DNA template (primer sequence, 5′-ATTTGAACTACATCATGGTT-3′; template sequence, 5′-GATGATCTAGCACAACCATGATGTAGTTCAAAT-3′). Reactions were initiated by the addition of enzyme, and initial rates of DNA extension were determined by quantification of total DNA extension over time (0−9 min) using PAGE and autoradiography as described above. Initial rates of DNA polymerization were plotted as a function of inhibitor concentration to determine the inhibitory effect of CPHM.

Chelation of Mg^{2+} by the Inhibitor CPHM. Metal titration studies were performed in reaction buffer (pH 7.6) with CPHM at a concentration of 20 μM in a volume of 200 μL. Scans were corrected for buffer baseline absorbance and dilution during the titration. Scans were performed between 250 and 450 nm for successive 1 μL additions of $MgCl_2$ (0−70 mM final concentration). The absorbance at 350 nm was used for quantitation of the fraction of chelated CPHM. Data were fit to the equation $[I{\cdot}Mg^{2+}] = [I_T][Mg^{2+}]/([Mg^{2+}] + K_d)$, where $[I_T]$ is the total concentration of CPHM in the titration mixture.

RESULTS

Effect of CPHM on DNA Strand Transfer. A model DNA strand transfer assay system (Figure 1) was used to study CPHM inhibition of HIV-1 RT-catalyzed DNA strand transfer. A DNA acceptor template was used in these experiments. While in vivo the minus strand DNA strand transfer reaction uses RNA as an acceptor template, the second, plus strand DNA transfer occurs onto a DNA template. Examination of strand transfer reactions using either DNA or RNA acceptor templates shows little or no kinetic difference (unpublished observation). For practical purposes, DNA was chosen to serve as the acceptor template in these experiments.

Figure 2A shows a PAGE gel autoradiogram of three representative reaction time courses at 0, 2.5, and 25.0 μM CPHM. The concentration dependence of DNA strand transfer inhibition by CPHM is depicted in Figure 2B. DNA strand transfer is slow compared to DNA polymerization (*5*, *46*) and occurs over the course of several minutes. Under the conditions that were used, DNA polymerization is rapid and essentially complete by the first time point (1 min). The primary DNA product is the nascent DNA that has been extended from the DNA primer to the end of the RNA template before it is transferred to the DNA acceptor template. CPHM inhibits the production of the DNA strand transfer product in a concentration-dependent fashion, displaying an IC_{50} of 2.2 μM.

After polymerization out to the end of a template, RT has the ability to incorporate an extra non-template-directed nucleotide at the end of the primary DNA product (*5*, *50*, *51*). This is called blunt-end nucleotide addition, and is a common feature of DNA strand transfer reactions (*51*). Blunt-end addition resulting in a misincorporation in the DNA strand transfer product at the strand transfer junction has been observed in model systems and during MLV replication (*51*, *52*). At the IC_{50} for strand transfer inhibition, CPHM inhibits blunt-end nucleotide addition, and inhibition is complete at concentrations of >25.0 μM. Thus, there appears to be a kinetic correlation between the inhibition of DNA strand transfer and blunt-end nucleotide addition reactions.

At higher CPHM concentrations, some pausing was detected during the first DNA·RNA extension as seen in Figure 2A. However, these pauses are relieved as the time course progresses and are not observed at CPHM concentrations around the IC_{50} for strand transfer inhibition. This observation indicates that the DNA pausing caused by CPHM is not a kinetically competent mechanism for explaining the inhibition of DNA strand transfer. Although this pausing was observed during RNA·DNA extension before strand transfer, it was not clear whether CPHM could inhibit DNA·DNA extension after strand transfer. An experiment was performed to determine whether CPHM inhibits RT-catalyzed DNA·DNA extension of the DNA strand transfer intermediate (Figure 1) and whether that contributes to overall strand transfer inhibition. For this assay, a DNA·DNA template·primer system consisting of the primary DNA product annealed to the DNA acceptor template was utilized. Little pausing was observed at the IC_{50} for strand transfer inhibition (data not shown), underscoring the conclusion that pausing during DNA synthesis by RT does not contribute significantly to the observed inhibition of strand transfer product formation.

HIV-1 nucleocapsid protein has been shown previously to be able to enhance DNA strand transfer reactions catalyzed by HIV-1 RT (*12*, *20*−*23*, *26*, *46*). Previous observations with another DNA strand transfer inhibitor, actinomycin D, indicated that HIV-1 nucleocapsid protein (NC) can shift the IC_{50} of actinomycin D inhibition of DNA strand transfer (*46*, *48*). NC was tested in the same manner to determine if it would have an effect on CPHM inhibition similar to that of strand transfer. NC was added to a final concentration of 1 μM to the reaction mixtures, which has previously been found to be the optimum concentration for enhancing DNA strand transfer. The IC_{50} for inhibition in the presence of NC is 2.0 ± 0.2 μM (data not shown), the same value as in the absence of NC. NC has no effect on CPHM inhibition of DNA strand transfer.

To begin to evaluate the mechanism of binding of CPHM to RT, two analogues, 4-chlorophenyhydrazone of pyruvic acid (CPHP) and 4-chlorophenylhydrazone of acetone (CPHA) (Scheme 1), were synthesized in an attempt to determine

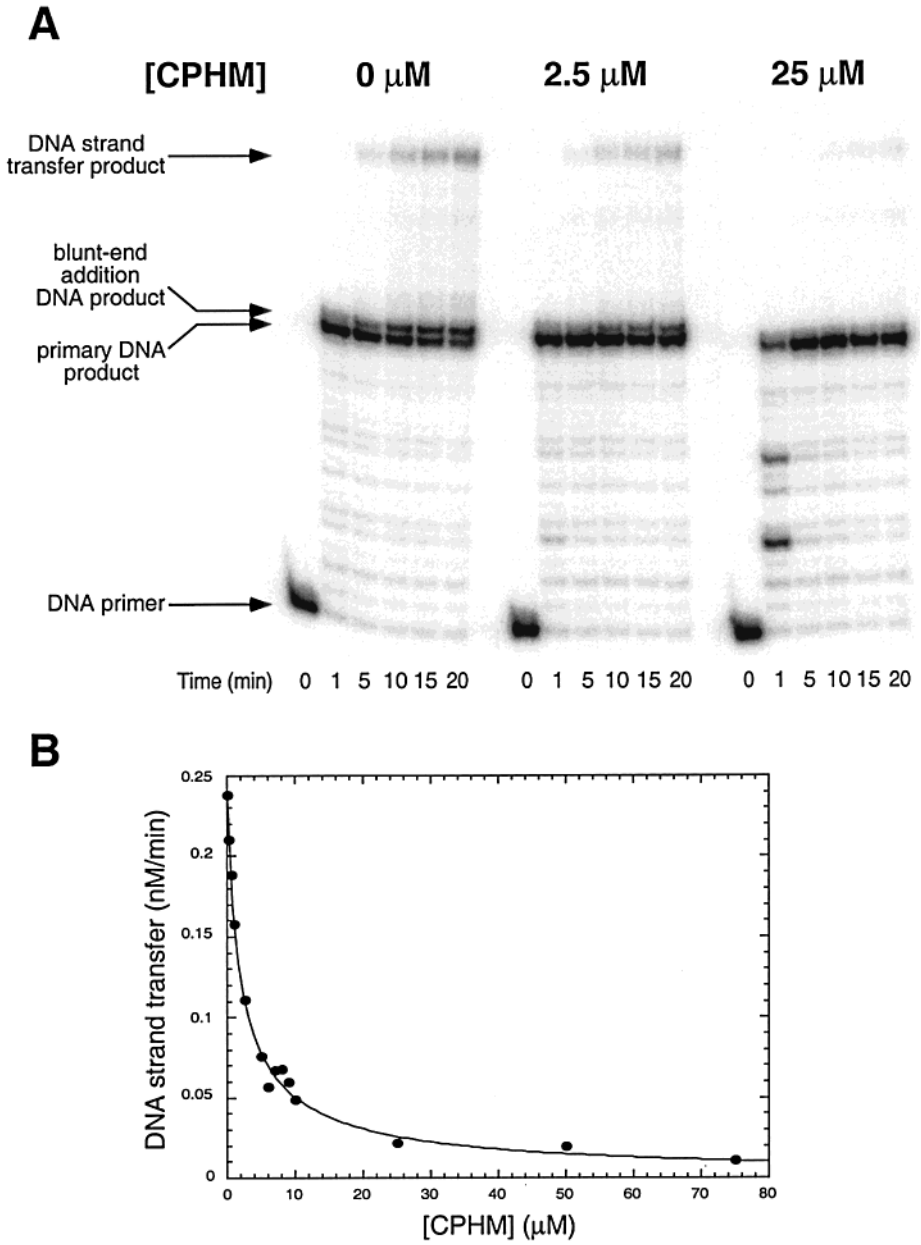

FIGURE 2: Effect of CPHM on DNA strand transfer. Reactions were performed as described in Materials and Methods with increasing amounts of CPHM at final concentrations of 0, 0.25, 0.5, 1.0, 2.5, 5.0, 6.0, 7.0, 8.0, 9.0, 10.0, 25.0, 50.0, and 75.0 μM with stoichiometric concentrations of RT and the template·primer complex (20 nM) and 400 nM DNA acceptor. CPHM was added after the addition of all other components during the preincubation. After initiation with 10 mM $MgCl_2$/0.1 mM dNTPs, samples were withdrawn at 0, 1, 5, 10, 15, and 20 min and analyzed by PAGE. (A) Gel analysis of DNA strand transfer products in the presence of CPHM. Representative autoradiogram of three reaction time courses (0, 2.5, and 25 μM CPHM). The amount of DNA strand transfer product was quantitated by phosphorimager analysis, and initial rates were determined. (B) The concentration dependence of DNA strand transfer inhibition by CPHM is shown. DNA strand transfer activity (nanomolar per minute) is plotted as a function of the total concentration of CPHM. The data were fit to the equation % activity $= A_{max}/[1 + ([CPHM]/IC_{50})^n]$. The IC_{50} for CPHM inhibition of DNA strand transfer was calculated to be 2.2 $\pm$ 0.2 μM.

the importance of the dicarboxylic acid moiety of CPHM. These compounds were synthesized as described in Materials and Methods and tested as described in Figure 2. No inhibition of strand transfer or DNA polymerase pausing was detected with either CPHP or CPHA at concentrations of $\leq$200 and $\leq$30 μM, respectively (data not shown).

Effect of CPHM on HIV-1 RT RNase H Activity. For strand transfer to occur, the primary extended DNA product must be available to anneal to the DNA acceptor template to form the strand transfer intermediate (Figure 1). It is not known whether this intermediate step occurs in the absence of proteins or in a higher-order complex with RT and/or other HIV proteins. At least a portion of the primary extended DNA product at some point must be single-stranded. For this to occur, the RNase H activity of HIV-1 RT must hydrolyze portions of the 5′-end of the RNA to make the primary extended DNA product competent for transfer. It has been observed previously that this RNase H activity is the rate-limiting step of DNA strand transfer in vitro (*5*). CPHM was tested to determine its capability for inhibiting RT RNase H that would in turn contribute to strand transfer inhibition. The RT RNase H assay (Figure 3) was completed under strand transfer conditions as described in Materials and Methods except that the RNA template strand was radiolabeled. Figure 3 depicts three representative reaction time courses at 0, 2.5, and 25.0 μM CPHM and graphs

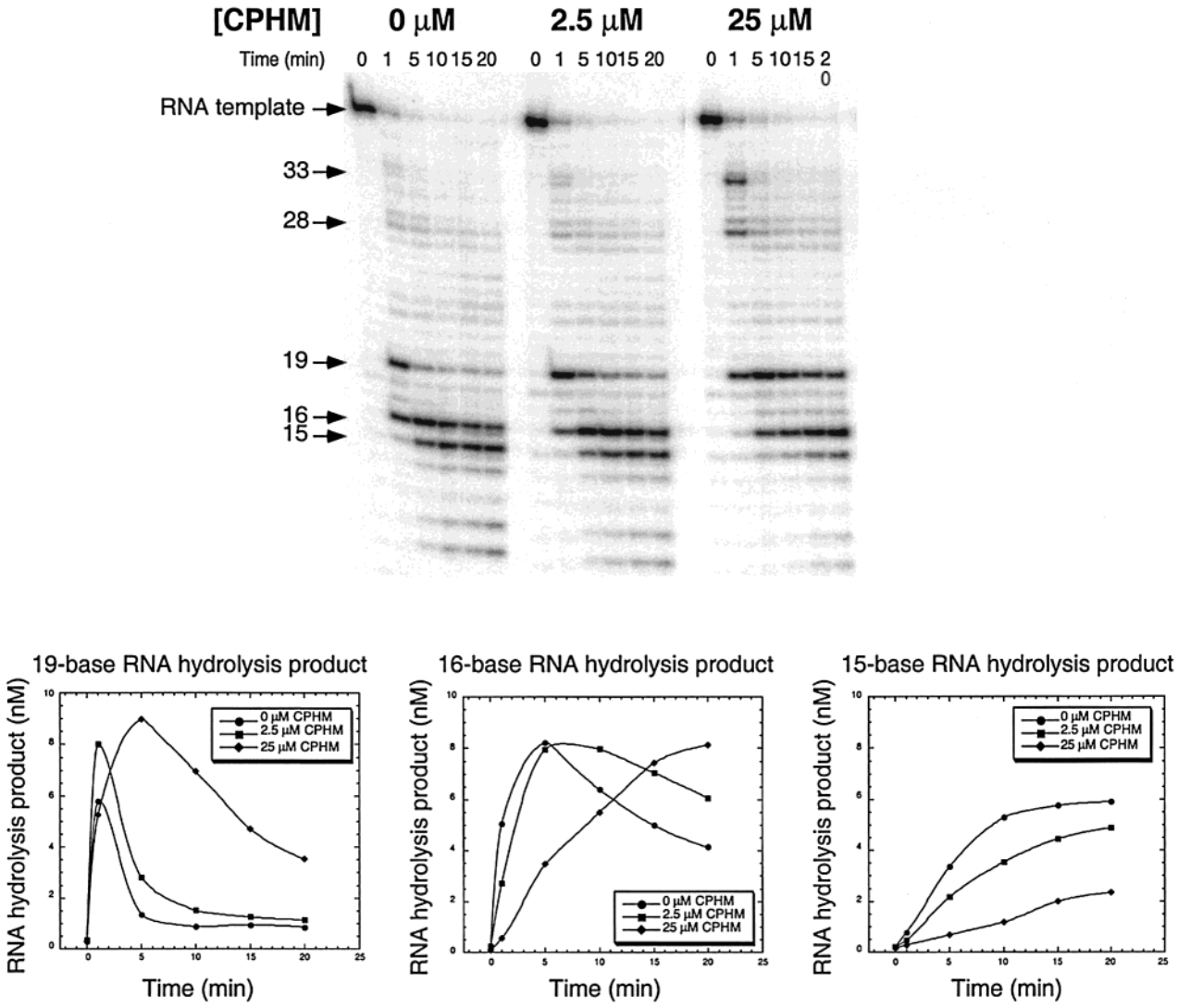

FIGURE 3: Effect of CPHM on HIV-1 RT RNase H activity during strand transfer. Reactions were performed as described in the legend of Figure 2. A representative PAGE autoradiogram of three reaction mixtures containing 0, 2.5, and 25.0 μM CPHM and the graphs of the reaction progress curves for the 19-, 16-, and 15-base RNA cleavage products are shown. The amounts of RNA hydrolysis products were quantitated by phosphorimager analysis, and the initial rates of the 15-mer RNA hydrolysis product were used to generate an IC_{50} for CPHM inhibition of RT RNase H (4.5 ± 0.3 μM).

showing the accumulation pattern of the three most prominent RNA hydrolysis products. Upon addition of CPHM, the accumulation pattern of RNA cleavage products changes. In the absence of CPHM, the RNA template is cleaved down to a 19- and 16-mer RNA product by 1 min and is then cleaved to 16- and 15-base RNA products which subsequently give rise to smaller RNA cleavage products. With increasing amounts of CPHM, the lifetimes of the longer RNA products are increased as represented graphically in Figure 3, indicating that the RNase H activity hydrolyzes these RNA intermediates more slowly. It is especially evident that the 19-base RNA intermediate accumulates as seen most clearly at 25.0 μM CPHM (Figure 3). Also, at high concentrations, larger RNA products (28- and 33-base RNAs) become apparent, suggesting two possible mechanisms of RNase H inhibition depending on the concentration of inhibitor used. However, the 28- and 33-base RNA products do turn over to smaller products as the reaction course proceeds. Closer examination of the cleavage locations indicates that these larger RNA products correlate with polymerase pausing (Figure 2 and below). To obtain an inhibition IC_{50} for RNA hydrolysis in the presence of CPHM, the rate of 15-base product appearance was plotted as a function of CPHM concentration. This inhibition is consistent with DNA strand transfer inhibition, with an IC_{50} of 4.5 μM. This IC_{50} should be regarded as an upper limit since only one hydrolysis product was monitored. Importantly, the time scale of the change in the RNA hydrolysis pattern correlates with the time scale of strand transfer inhibition. This is in contrast to the small amount of polymerase pause intermediates that do subsequently turn over to full-length primary DNA extension products early in the strand transfer reaction time course. At 75.0 μM, CPHM inhibits the rate of 15-mer appearance by ~91%, consistent with the extent of inhibition for strand transfer as observed in Figure 2.

The conditions in the RNA hydrolysis experiment in Figure 3 represent stoichiometric concentrations of RT with respect to the template·primer complex. The 19-base RNA product is formed rapidly in the presence of stoichiometric amounts of the enzyme and template·primer complex (Figure 3) and under steady-state conditions where a template·primer complex is in 10-fold excess over enzyme (Figure 4). This

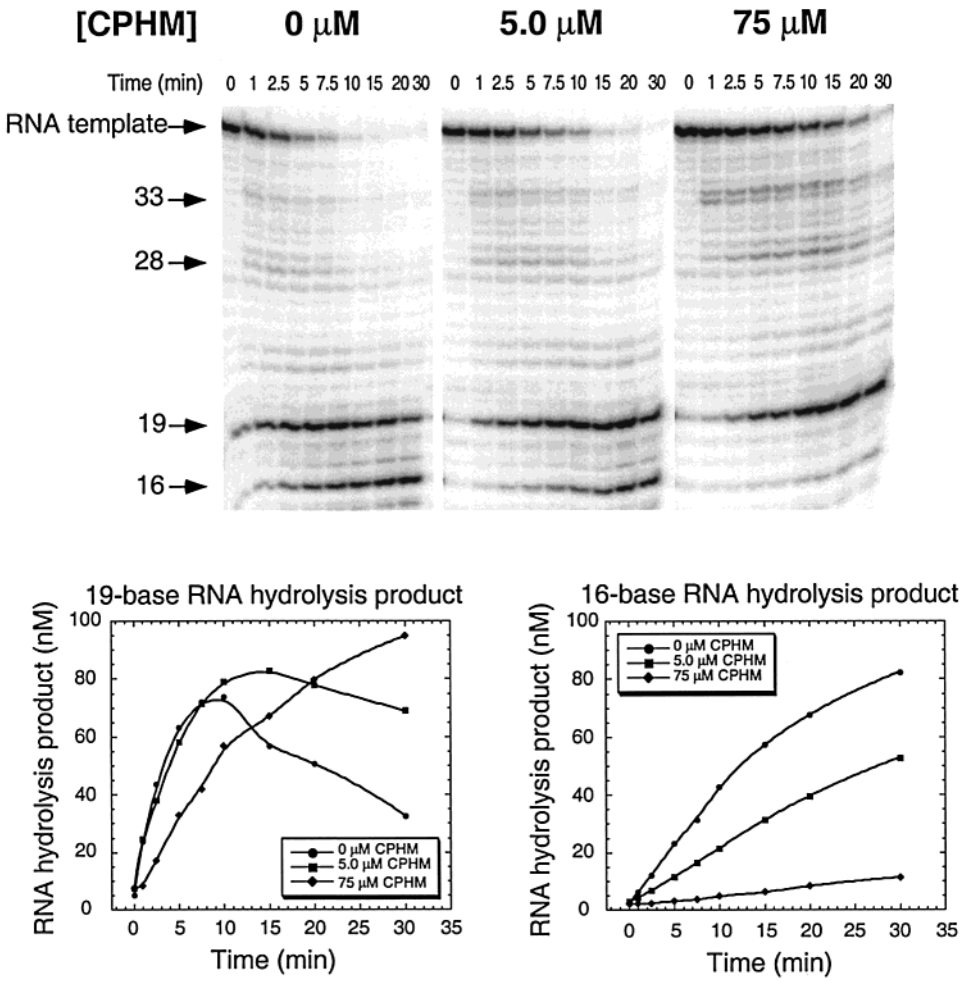

FIGURE 4: Effect of CPHM on HIV-1 RT RNase H activity under steady-state reaction conditions. The reactions were completed as described in Materials and Methods with increasing amounts of CPHM at final concentrations of 0, 0.5, 1.0, 2.5, 5.0, 7.5, 10.0, 25.0, 50.0, and 75.0 μM. The concentrations of RT, the template·primer complex, and the acceptor template are 20 nM, 200 nM, and 4 μM, respectively. Time points were 0, 1, 2.5, 5, 7.5, 10, 15, 20, and 30 min. A representative PAGE autoradiogram of three reaction mixtures containing 0, 5.0, and 75.0 μM CPHM and the graphs of the reaction progress curves for the 19- and 16-base RNA cleavage products are shown.

suggests that CPHM does not significantly inhibit the formation of the 19-base RNA product. However, the turnover of the 19-base RNA product to the 16-base, 15-base, and smaller RNA products was inhibited in a concentration-dependent fashion. The magnitude and kinetics of this inhibition are consistent with inhibition of DNA strand transfer by CPHM.

The direct examination of the inhibition of polymerase-independent RNase H activity was examined by preforming the 40-base DNA·RNA primary extension product (Figure 1) and examining the rate of RNA hydrolysis in the absence of added dNTPs and increasing amounts of CPHM. The pattern of RNA cleavage under these conditions was similar to that seen during DNA strand transfer reactions (Figure 3) with an IC_{50} of 3.0 μM (data not shown and ref *39*), in close agreement with the IC_{50} for DNA strand transfer of 2.2 μM. This result supports the hypothesis that CPHM primarily targets the polymerase-independent RNase H activity during DNA strand transfer reactions.

E. coli RNase H is very similar in its structure and activity to the RNase H domain of HIV-1 RT (*38*). To determine whether the inhibition of RT RNase H activity is specific for the RNase H domain, CPHM was tested for its capability to inhibit *E. coli* RNase H. The experiment was conducted as described in Materials and Methods with increasing amounts of CPHM added to the reaction time courses. CPHM was found to inhibit *E. coli* RNase H in a fashion similar to that with the RT RNase H activity with an IC_{50} of 2.6 $\pm$ 0.6 μM (data not shown). This IC_{50} is similar to that found for HIV-1 RT RNase H inhibition in the absence of dNTP incorporation (3.0 μM; see above).

Importantly, CPHM had a similar affect on *E. coli* RNA hydrolysis by changing the accumulation pattern of RNA hydrolysis products as observed for RT RNase H hydrolysis in Figures 3 and 4. However, there was no correlation of cleavage patterns between *E. coli* and HIV-1 RT RNase H.

Effect of CPHM on the Pre-Steady-State Kinetics of dTTP Incorporation and RNA Hydrolysis. Both DNA strand transfer and RNA hydrolysis are slow processes that occur over several minutes, with the rate-limiting step of strand transfer being the rate of RNA hydrolysis catalyzed by HIV-1 RT. However, the DNA strand transfer and RNase H assays shown in Figures 2−4 do not address events that occur during single nucleotide incorporation and early RNA cleavage, events that occur within the first few seconds of the reaction. Since the polymerase and RNase H domains of HIV-1 RT have been shown to be spatially and temporally coupled to each other with a footprint of 18 or 19 bases

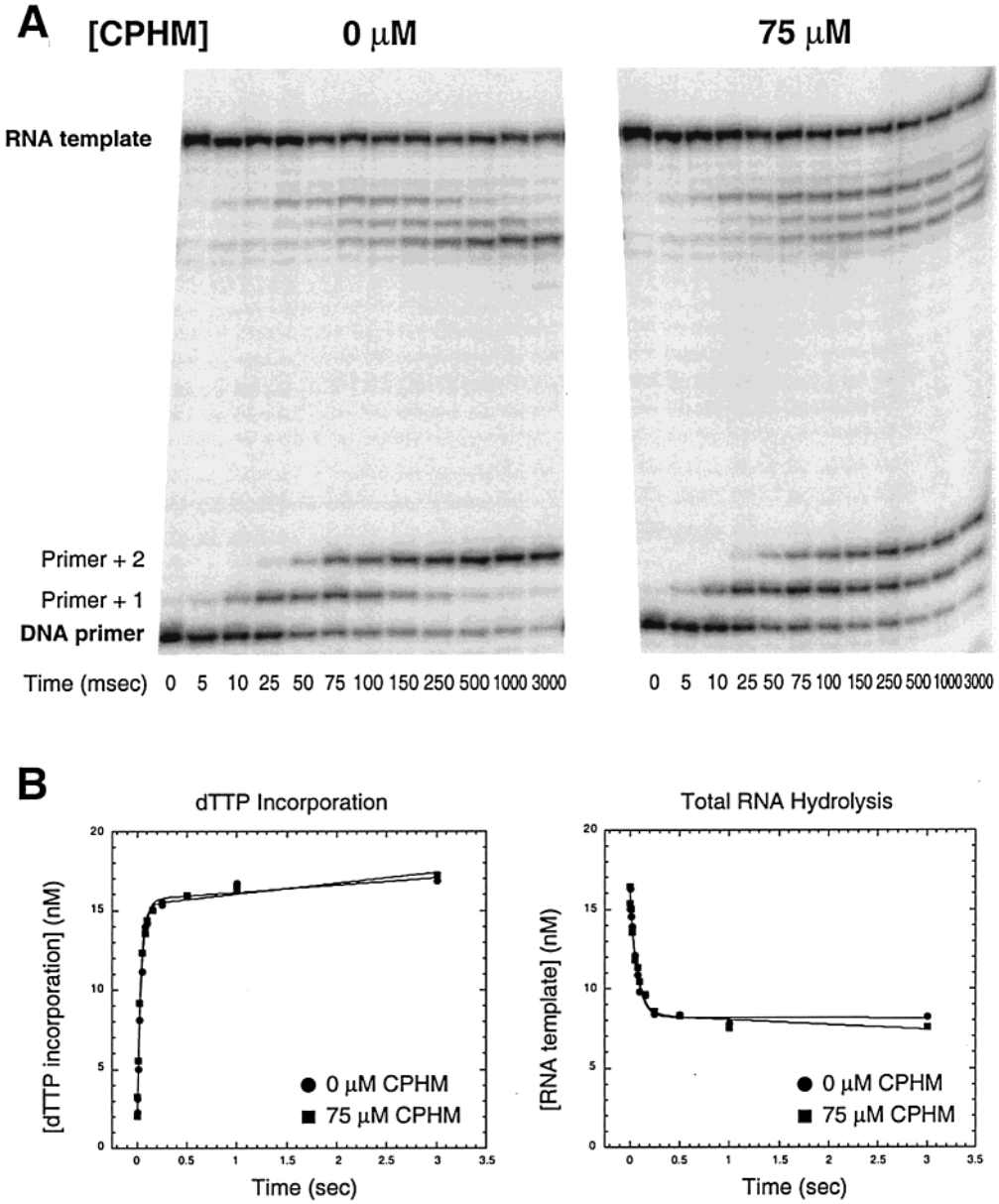

FIGURE 5: Effect of CPHM on pre-steady-state kinetics of dTTP incorporation and RNA hydrolysis. Reactions were performed as described in Materials and Methods in the presence of final concentrations of CPHM of 0 or 75.0 μM (added during preincubation), 30 nM RT, 20 mM template·primer complex, 10 mM $MgCl_2$, and 0.1 mM dTTP and in the absence of DNA acceptor. The reactions were carried out with a doubly labeled template·primer complex to observe simultaneous RNA hydrolysis and dTTP incorporation. Time points were 0, 5, 10, 25, 50, 75, 100, 150, 250, 500, 1000, and 3000 ms. (A) Gel analysis of RNA hydrolysis and dTTP incorporation products. RNA hydrolysis and dTTP incorporation product amounts were quantitated as described in the legend of Figure 3, and pre-steady-state rates were determined. (B) Graphical analysis of dTTP incorporation and total RNA hydrolysis. The burst rates for dTTP incorporation are 30.7 $\pm$ 4.2 and 38.2 $\pm$ 4.7 for 0 and 75.0 μM CPHM, respectively.

between these two active sites (*3*, *4*, *6*−*8*), pre-steady-state analysis of single- or double-nucleotide incorporation and concomitant RNA hydrolysis during RNA·DNA extension is possible. An important question concerns whether CPHM inhibits the catalysis of nucleotide incorporation and RNA hydrolysis by RT or whether it elicits its effect on some other step during DNA synthesis and RNA hydrolysis, such as inhibiting DNA·RNA duplex translocation. The inhibition of duplex translocation by CPHM could result in both the observed pausing during DNA synthesis at high concentrations of inhibitor and the change in RNA hydrolysis product accumulation during RNase H cleavage by RT. To address these questions, we conducted a double-labeling experiment where single-nucleotide incorporation and initial RNA hydrolysis events could be observed simultaneously and the products correlated with each other. Extension of the DNA by two nucleotides and concomitant RNA cleavage were monitored under single-turnover conditions. In Figure 5A, a PAGE autoradiogram of the reaction time courses in the presence of 0 and 75.0 μM CPHM is shown. The difference in lengths of the DNA primer and RNA template with their respective nucleotide incorporation and RNA hydrolysis products allows for the simultaneous resolution of DNA and RNA products. Due to the nature of the RNA template sequence (see Figure 5B), two dTTPs are incorporated. A graphical analysis of double-dTTP incorporation and total RNA hydrolysis is presented in Figure 5B. At the early time points of the reaction (0−100 ms), little difference is seen

in either dTTP incorporation or total RNA hydrolysis. The pre-steady-state burst rate at 0 and 75.0 μM CPHM is 30.7 $\pm$ 4.2 and 38.2 $\pm$ 4.7 s^{-1}, respectively. No difference in the extent of total (two nucleotides) dTTP incorporation or total RNA hydrolysis is observed even at a very high concentration of CPHM, 75.0 μM, which is ~35-fold above the IC_{50} for strand transfer and 17-fold above that for RT RNase H inhibition. However, as seen in the autoradiogram, the pattern of dTTP incorporation and RNA hydrolysis is somewhat different in the absence and presence of 75.0 μM CPHM. The apparent extension of the singly extended primer by a second nucleotide, as well as the turnover of the 36-base RNA hydrolysis product to the 35- and 34-base RNA product, displays similar initial rates at 75.0 μM. However, the extent of second-nucleotide incorporation and hydrolysis is smaller than in the absence of CPHM. This suggests that CPHM can act to inhibit the translocation of the DNA·RNA template·primer complex at high concentrations of CPHM without affecting the initial catalytic events of nucleotide incorporation or RNA hydrolysis.

This experiment also conclusively shows that CPHM has no effect on the binding of the DNA template·primer complex to the enzyme. If CPHM bound enzyme, or alternatively bound DNA substrate, and prevented its binding to the enzyme active site, a pronounced reduction in the burst amplitude would be observed. Under these experimental conditions, the product burst amplitude corresponds to the concentration of the enzyme−template·primer complex present at the initiation of the reaction. Figure 5B shows that the burst amplitudes for both the polymerase and RNase H activities of HIV-1 RT are identical in reaction mixtures containing 0 or 75 μM CPHM. Due to the lack of change in the burst amplitude, at inhibitor concentrations that are >30-fold greater than the observed IC_{50} for strand transfer inhibition, we conclude that CPHM does not inhibit by interfering directly with template·primer binding.

Specificity of Inhibition by CPHM. Inhibition by CPHM was found to be highly specific for HIV-1 reverse transcriptase. Two other reverse transcriptases were assayed using the DNA strand transfer assay (Figure 1). Inhibition of DNA strand transfer of AMV reverse transcriptase by CPHM had an IC_{50} of >68 μM, while the same assay with M-MLV reverse transcriptase showed no detectable inhibition of strand transfer at ≤100 μM CPHM. No inhibition was detectable when the DNA polymerase activities of Klenow fragment or T4 DNA polymerase were examined with CPHM concentrations of ≤75 μM.

Binding of Mg^{2+} to CPHM. The UV−visible spectrum of CPHM is shown in Figure 6. The spectrum of CPHM alone has an absorbance maximum of 335 nm and a minor shoulder peak centered at 305 nm. Upon addition of $MgCl_2$, the maximum absorbance is shifted to higher wavelengths, with a new maximum at 345 nm. In addition, the metal-chelated CPHM displays an ~15% increase in its extinction coefficient. When the change in absorbance at 350 nm was monitored, the constant for dissociation of Mg^{2+} binding to CPHM was determined to be 2.8 $\pm$ 0.1 mM (Figure 6). Thus, under DNA strand transfer reaction conditions (10 mM Mg^{2+}), ~80% of the CPHM is chelated to Mg^{2+}.

The pyruvic acid analogue CPHP was also tested for its ability to bind Mg^{2+}. Titrations with metal concentrations of ≤70 mM showed no evidence of metal·CPHP chelation as evidenced by the lack of change in the UV−visible spectrum of CPHP (data not shown).

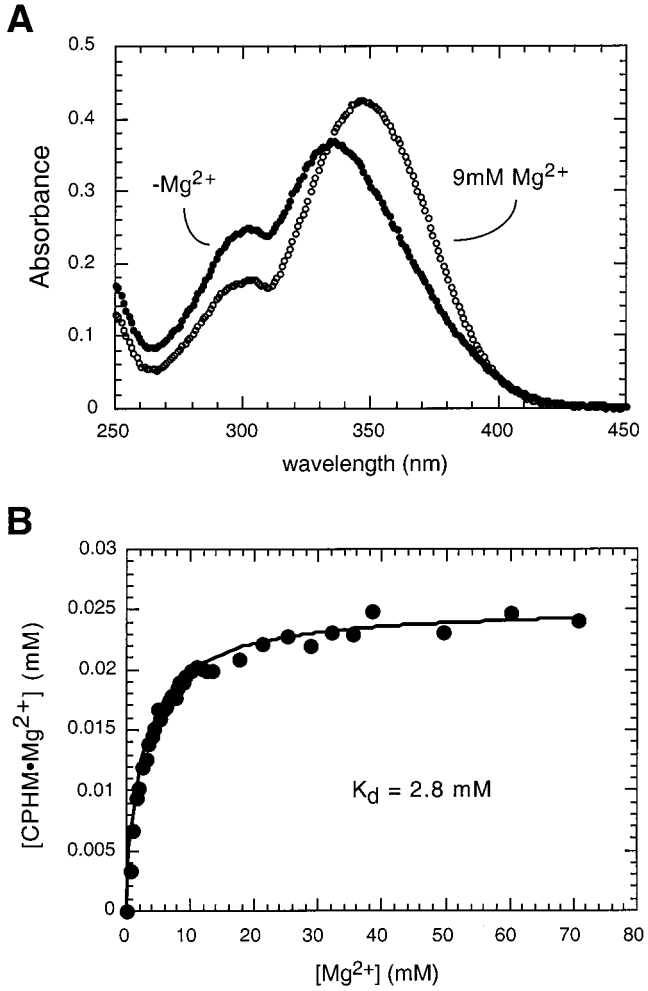

FIGURE 6: Chelation of Mg^{2+} by the inhibitor CPHM. (A) UV−visible spectrum of CHPM and its Mg^{2+} chelate. Spectra are presented of CPHM alone (○) or in the presence of 9 mM $MgCl_2$ (●). A change in A_{max} from 335 to 345 nm and a ~15% increase in the extinction coefficient were observed upon addition of Mg^{2+}. (B) Titration reactions were performed as described in Materials and Methods. Titrations were performed by successive addition of $MgCl_2$ while the absorbance of CPHM was monitored at 350 nm.

DISCUSSION

Here we describe the kinetic characterization of a newly identified inhibitor of HIV-1 RT, 4-chlorophenylhydrazone of mesoxalic acid (CPHM). In previous reports (*45*, *46*), we have described a novel approach for inhibiting HIV-1 replication, which is targeting DNA strand transfer with chemical inhibitors. While many inhibitors that target reverse transcriptase act by inhibiting the DNA polymerase activity of the enzyme, inhibitors that target strand transfer could be useful as potential therapeutic agents as well as useful tools for understanding the mechanism of DNA strand transfer.

CPHM was identified in an automated screen of a chemical compound library for compounds that would inhibit the process of DNA strand transfer (*45*). Through model in vitro DNA strand transfer and RNase H assays, we have characterized the mechanism of inhibition of DNA strand transfer reactions by CPHM. There are several steps during strand transfer during which CPHM could target which would result

in the observed strand transfer inhibition: the RNA-dependent DNA polymerization step catalyzed by RT, RT RNase H activity, the intermediate annealing or exchange step, and the DNA-dependent DNA polymerization step also catalyzed by RT. Inhibition at any one or more of these steps could contribute to the overall inhibition of DNA strand transfer.

We provide evidence here that CPHM inhibits DNA strand transfer by targeting the RNase H activity of RT, disrupting the translocation or repositioning of the enzyme on the RNA·DNA duplex, and inhibiting the necessary hydrolysis of RNA intermediates required for strand transfer. While some pausing during DNA synthesis was observed in the presence of high CPHM concentrations, this inhibition could not sufficiently explain the overall kinetics of DNA strand transfer inhibition.

CPHM inhibits the initial catalysis of neither nucleotide incorporation nor RNA hydrolysis (Figure 5), suggesting that DNA synthesis as well as the chemistry step of RNA hydrolysis remains functional during DNA strand transfer in the presence of CPHM. It is most likely that the slowing of nucleotide incorporation and RNA hydrolysis turnover, observed at high CPHM, is due to CPHM retarding the translocation of RT along the RNA·DNA substrate as opposed to inhibiting initial catalytic events. However, since this effect requires high inhibitor concentrations, this inhibition is a secondary target of CPHM and not the predominant mechanism.

The ability of CPHM to inhibit the intermediate or annealing step of strand transfer was also tested. A modified version of the assay described by Davis et al. (unpublished data) was used to determine if CPHM could inhibit the annealing of the primary DNA extension product to the acceptor template. CPHM had no effect on DNA·DNA annealing even at concentrations of $\leq$75.0 μM CPHM. This might explain why nucleocapsid protein had no effect on the inhibition of strand transfer by CPHM. Recent studies have shown that actinomycin D inhibits DNA strand transfer reactions by strongly inhibiting this annealing step and that NC protein could help to relieve some of this inhibition in strand transfer (*46*, *48*). These studies also show that actinomycin D has no effect on the RNase H activity of HIV-1 RT (*46*−*48*). This difference in NC sensitivity and the observation that CPHM targets the RNase H activity of HIV-1 RT points to a difference between actinomycin D and CPHM in their mechanisms of inhibition.

From Figures 3 and 4, it is apparent that CPHM has a pronounced effect on the RNase H hydrolysis activity of RT. Although CPHM has little effect on total RT-catalyzed RNA hydrolysis, it abruptly changes the distribution of the RNA hydrolysis products produced in the absence of DNA synthesis. Some accumulation of longer RNA hydrolysis products (28- and 33-base RNAs) is observed, however, only at high CPHM concentrations. Also, the 28- and 33-base RNA products are the result of polymerase-dependent RNA hydrolysis by RT, which occurs during DNA synthesis, and correlates well with the first-extension DNA pausing also seen at high CPHM concentrations (Figures 3, 4, and 7B). The RNase H inhibition consistent with strand transfer inhibition only occurs after primary DNA synthesis has finished.

In our assay, RT has first been bound to the RNA·DNA template·primer complex in the presence of CPHM. After reaction initiation with nucleotides and Mg^{2+}, RT quickly extends the nascent DNA from the DNA primer to the end of the RNA template (Figure 7A). During this first extension, the polymerase-dependent RNase H activity of RT cleaves the RNA template periodically and with little specificity. Once DNA polymerization ends as RT reaches the 5′-end of the RNA template, the RNase H activity of RT makes an initial cleavage of the RNA to produce a predominant 19-base RNA product. At that point, RT must reposition, or translocate, the RNA·DNA duplex so as to position the RNase H domain further toward the 5′-end of the RNA template to process the 19-base RNA down to smaller RNA products (16- and 15-base RNAs). This places the 3′-end of the DNA out of the polymerase active site. A similar translocation must occur for correct positioning of the DNA·RNA duplex for the blunt-end nucleotide (Figure 7A). The inhibition of the polymerase-independent RNase H and blunt-end nucleotide addition activities are consistent with the role of CPHM in interfering with this substrate repositioning.

Whether this repositioning occurs by RT "sliding" on the RNA·DNA duplex or by RT disassociating from the duplex and then rebinding is not known. HIV-1 RT RNase H has been shown to be slightly processive (*53*), suggesting that some sliding of the DNA·RNA duplex occurs. Either mechanism must encompass RT binding in a thermodynamically unfavorable binding mode for RT translocation and subsequent strand transfer to occur. Since the processing of the 5′-end of the RNA template is very slow and is the rate-limiting step of strand transfer, it is therefore logical to conclude that translocation is, in itself, an inefficient process. The current data suggest that CPHM causes this already inefficient and slow process of translocation to become even more inefficient, thereby further slowing the rate-limiting step of strand transfer.

Identification of an RNase H inhibitor is very significant, since examples of potent inhibitors of HIV-1 RT RNase H activity are few (*45*). The identification of the metal chelator (BBNH) (*44*), however, has raised the possibility that the dicarboxylic acid plays an important role in RNase H/translocation disruption by chelating RNase H active site Mg^{2+}. Consistent with this hypothesis, both CPHP, which lacks one carboxylic acid, and CPHA, which lack both, display no inhibition in strand transfer, suggesting that the dicarboxylic acid must be retained for inhibitor activity.

Keck et al. proposes an activation/attenuation model for the metal dependence of RNase H activity, suggesting that only one divalent metal is required for hydrolysis and a second metal then inhibits the enzyme after the initial hydrolysis, thus attenuating the enzyme (*54*).

Several possible orientations of RT binding to RNA·DNA heteroduplex substrates, with respect to positioning of the RNase H and polymerase domains, have been proposed (*55*−*58*). It is possible that CPHM prevents access to one or more of these binding modes necessary for polymerase-independent RNase H hydrolysis to occur. This would restrict RT from hydrolyzing RNA into smaller products after the initial cleavage.

The actual binding site(s) of CPHM is not known. However, since CPHM affected *E. coli* RNase H in the same manner as HIV-1 RT RNase H, by inhibiting the turnover of long RNA hydrolysis products into smaller products, it is reasonable to hypothesize that CPHM binds in the RNase H

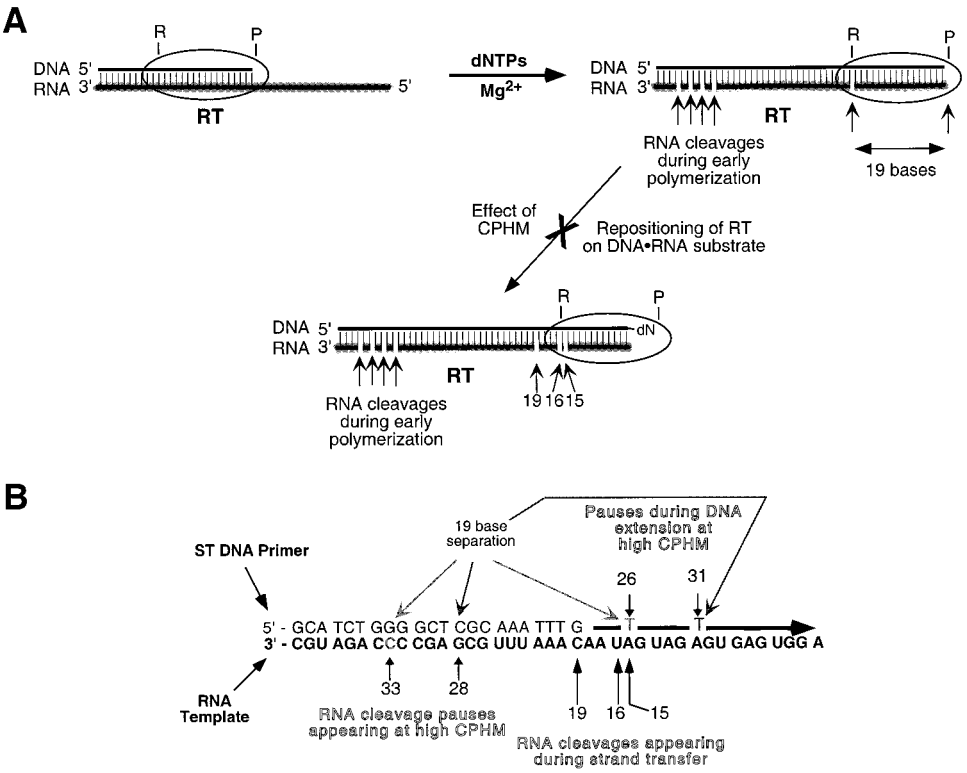

FIGURE 7: Model for the effect of CPHM on the translocation of HIV-1 RT RNase H. A schematic representation of how CPHM affects the translocation activity of RT RNase H is shown. The prereaction initiation, first DNA extension/polymerase-dependent RNA hydrolysis, and polymerase-independent/repositioning steps are shown. Before reaction initiation, RT (oval) is bound to the template (RNA, bold line)•primer (DNA) complex. The relative positions of the polymerase domain (P) and the RNase H domain (R) with respect to nucleic acid substrate binding are indicated. RNA cleavages and sizes of RNA hydrolysis products are indicated by arrows. (B) The sequences of the oligonucleotide substrates used in DNA strand transfer and RNase H activity assays are shown. The boldface sequence represents the RNA template, and the lightface sequence represents the DNA primer. For clarity, the DNA acceptor template is not shown. Arrows pointing to the DNA that is extended off of the DNA primer indicate paused DNA products that accumulate at high CPHM concentrations. Arrows pointing directly to the RNA template on the left side indicate RNA products that also accumulate at high CPHM concentrations. The highlighted bases represent the 19-base difference that can be seen when correlating RNA hydrolysis and DNA extension in the presence of CPHM.

domain of HIV-1 RT. The structures of *E. coli* RNase H (*59*−*61*), the RNase H domain of HIV-1 RT (*62*), and the HIV-1 RT (*6*−*8*) have been determined. The overall folds of the RNase H domain of HIV-1 RT and the *E. coli* RNase H are quite similar (*62*). Furthermore, the geometrical alignments of secondary structure elements in the *E. coli* RNase H and the RNase H domains of HIV-1, M-MLV, and AMV reverse transcriptases reveal significant amino acid and predicted structural homology (*62*−*64*). The similarities in sequence and structure between these RNase H domains and the *E. coli* enzyme suggest that CPHM might act broadly in inhibiting RNase H activity. However, while CPHM inhibited *E. coli* RNase H, no inhibition of either M-MLV or AMV reverse transcriptases was observed under conditions where RNase H inhibition would be detected. Interestingly, amino acid alignments show that the sequence of M-MLV is more identical to the *E. coli* RNase H than the HIV-1 RNase H (*62*−*64*), but no inhibition of the M-MLV RT was detected.

Several factors my contribute to this observed specificity of CPHM for HIV-1 RT. It is possible that CPHM binds outside the RNase H domain of HIV-1 RT, in a region not conserved between the retroviral RTs. However, the sensitivity of the *E. coli* RNase H toward CPHM and its structural similarity to the RNase H domain of HIV-1 RT strongly support a similar binding mechanism. Alternatively, there may be important structural differences between the retroviral RNase H domains that give rise to the observed inhibitor specificity. Significantly, HIV-1 RT is a heterodimer composed of two subunits, both of which are involved in formation of single RNase H and polymerase active sites. M-MLV exists as a monomer in the absence of DNA, but is thought to form a dimer in the presence of a nucleic acid template•primer complex (*65*−*67*). In principle, this M-MLV dimer could consist of two functional RNase H domains. It is possible that one or both of these RNase H active sites may not bind CPHM. Recently, RSV RT was shown to be a dimer, but most of its polymerase and RNase H activity resides in the smaller α-subunit (*68*). Discerning which factors are involved in this specificity must await further enzyme structural and inhibitor structure−activity studies.

It is clear from initial structure−activity studies and metal binding experiments (Figure 6) that the dicarboxylic acid of CPHM moiety is essential for inhibitor activity. CPHM analogues lacking even one of the carboxylic acid groups (Scheme 1) displayed no inhibition of enzyme activity. This lack of inhibition correlates directly with the inability of CPHP (pyruvic acid hydrazone, Scheme 1) to chelate Mg^{2+}. On the other hand, metal titration experiments indicate that under the conditions of the DNA strand transfer reactions, the dicarboxylic acid inhibitor CPHM is nearly completely chelated to Mg^{2+} (Figure 6). This strong correlation between inhibitor activity and metal binding supports the hypothesis

that dicarboxylic acid−Mg^{2+} chelation is directly involved in inhibitor function.

It is possible that CPHM could inhibit by first chelating Mg^{2+} and then positioning itself with the extra metal in the active site which then could either (1) attenuate RNase H activity or (2) block the repositioning of RT on the RNA·DNA complex. This could also explain why CPHM exhibits little inhibition of initial RNase H cleavage, even at high concentrations, since the first initial RNA cleavages would occur regardless of the presence of the second metal atom. Biochemical and structural studies are currently underway to investigate this issue.

Inhibitors of RNase H activity such as CPHM, in combination with either strand transfer inhibitors that target a different step in strand transfer (*45*, *46*) or other inhibitors of RT or nucleocapsid function, could provide novel means for treating HIV-1 infection. It is possible that inhibitors such as CPHM that target the RNase H activity of HIV-1 RT could also inhibit important RNase H activity required for normal human cell function. If this is the case, then the usefulness of CPHM as a possible therapeutic agent might be compromised. In this case, comparative structure−activity and toxicity experiments would need to be implemented to increase the specificity of HIV-1 RT inhibition. However, many current dNTP analogue inhibitors of HIV-1 RT (i.e., AZT triphosphate) show some activity against cellular polymerases, with a corresponding level of toxicity. Still, these drugs play an important role in anti-HIV regimens. Furthermore, while CPHM exhibited inhibitory activity against *E. coli* RNase H activity, the specificity of inhibition by CPHM does not appear to be too broad since very little or no inhibition of M-MLV or AMV reverse transcriptases was observed. Future experiments in which the inhibition of human RNase H will be examined, as well as toxicity studies using viral culture assays, will help in addressing this possibility. Meanwhile, CPHM, a reasonably potent and specific inhibitor of HIV-1 RT RNase H, offers a new perspective on an old target of HIV-1 therapeutic intervention as well as valuable insights into a very important process of HIV-1 replication.

ACKNOWLEDGMENT

We thank Dr. Don Hupe (Parke-Davis Research Pharmaceuticals) for his continued support and insights and for providing the inhibitor PD126338 used in these studies.

REFERENCES

1. Temin, H., and Mizutani, S. (1970) *Nature 226*, 1211−1213.
2. Baltimore, D. (1970) *Nature 226*, 1209−1211.
3. Furfine, E. S., and Reardon, J. E. (1991) *J. Biol. Chem. 266*, 406−412.
4. Gopalakrishnan, V., Peliska, J. A., and Benkovic, S. J. (1992) *Proc. Natl. Acad. Sci. U.S.A. 89*, 10763−10767.
5. Peliska, J. A., and Benkovic, S. J. (1992) *Science 258*, 1112−1188.
6. Jacobo-Molina, A., Ding, J., Nanni, R. G., Clark, A. D., Lu, X., Tantillo, C., Williams, R. L., Kamer, G., Ferris, A. L., Clark, P., Hizi, A., Hughes, S. H., and Arnold, E. (1993) *Proc. Natl. Acad. Sci. U.S.A. 90*, 6320−6324.
7. Huang, H., Chopra, R., Verdine, G. L., and Harrison, S. C. (1998) *Science 282*, 1669−1675.
8. Kohlstaedt, L. A., Wang, J., Friedman, J. M., Rice, P. A., and Steitz, T. A. (1992) *Science 256*, 1783−1790.
9. Telesnitsky, A., Blain, S. W., and Goff, S. P. (1992) *J. Virol. 66*, 615−622.
10. Smith, C. M., Smith, J. S., and Roth, M. J. (1999) *J. Virol. 73*, 6573−6581.
11. Auxilien, S., Keith, G., Le Grice, S. F. J., and Darlix, J.-J. (1999) *J. Biol. Chem. 274*, 4412−4420.
12. Wu, T., Guo, J., Henderson, L. E., and Levin, J. G. (1999) *J. Virol. 73*, 4794−4805.
13. Cirino, N. M., Cameron, C. E., Smith, J. S., Rausch, J. W., Roth, M. J., Benkovic, S. J., and Le Grice, S. F. J. (1995) *Biochemistry 34*, 9936−9943.
14. Telesnitsky, A., and Goff, S. P. (1993) in *Cold Spring Harbor Monograph Series* (Skalka, A. M., and Goff, S. P., Eds.) pp 49−83, Cold Spring Harbor Laboratory Press, Cold Spring Harbor, NY.
15. Hu, W. S., and Temin, H. M. (1990) *Science 250*, 1227−1233.
16. DeStefano, J. J., Bambara, R. A., and Fay, P. J. (1994) *J. Biol. Chem. 269*, 161−168.
17. Canard, B., Sarfati, R., and Richardson, C. C. (1997) *Proc. Natl. Acad. Sci. U.S.A. 94*, 11279−11284.
18. Cameron, C. E., Ghosh, M., Le Grice, S. F., and Benkovic, S. J. (1997) *Proc. Natl. Acad. Sci. U.S.A. 94*, 6700−6705.
19. Allain, B., Lapadat-Tapolsky, M., Berlioz, C., and Darlix, J. L. (1994) *EMBO J. 13*, 973−981.
20. Peliska, J. A., Balasubramanian, S., Giedroc, D. P., and Benkovic, S. J. (1994) *Biochemistry 33*, 13817−13823.
21. DeStefano, J. J. (1996) *J. Mol. Biol. 271*, 16350−16356.
22. Guo, J., Henderson, L. E., Bess, J., Kane, B., and Levin, J. G. (1997) *J. Virol. 71*, 5178−5188.
23. You, J. C., and McHenry, C. S. (1994) *J. Biol. Chem. 269*, 31491−31495.
24. Tanchou, V., Gabus, C., Rogemond, V., and Darlix, J. L. (1995) *J. Mol. Biol. 252*, 563−571.
25. Rodriguez Rodriguez, L., Tsuchihashi, Z., Fuentes, G. M., Bambara, R. A., and Fay, P. J. (1995) *J. Mol. Biol. 270*, 15005−15011.
26. DeStefano, J. J. (1995) *Arch. Virol. 140*, 1775−1789.
27. Darlix, J. L., Vincent, A., Gabus, C., de Rocquigny, H., and Roques, B. (1993) *C. R. Acad. Sci., Ser. III 316*, 763−771.
28. Darlix, J. L., Lapadat Tapolsky, M., de Rocquigny, H., and Roques, B. P. (1995) *J. Mol. Biol. 254*, 523−537.
29. De Clercq, E. (1992) *AIDS Res. Hum. Retroviruses 8*, 119−134.
30. Wilson, J. E., Porter, D. J., and Reardon, J. E. (1996) *Methods Enzymol. 275*, 398−424.
31. Tucker, T. J., Lumma, W. C., and Culberson, J. C. (1996) *Methods Enzymol. 275*, 440−472.
32. Das, K., Ding, J., Hsiou, Y., Clark, A. D., Jr., Moereels, H., Koymans, L., Andries, K., Pauwels, R., Janssen, P. A., Boyer, P. L., Clark, P., Smith, R. H., Jr., Kroeger Smith, M. B., Michejda, C. J., Hughes, S. H., and Arnold, E. (1996) *J. Mol. Biol. 264*, 1085−1100.
33. Wu, J. C., Warren, T. C., Adams, J., Proudfoot, J., Skiles, J., Raghavan, P., Perry, C., Potocki, I., Farina, P. R., and Grob, P. M. (1991) *Biochemistry 30*, 2022−2026.
34. Spence, R. A., Kati, W. M., Anderson, K. S., and Johnson, K. A. (1995) *Science 267*, 988−993.
35. Palaniappan, C., Fay, P. J., and Bambara, R. A. (1995) *J. Biol. Chem. 270*, 4861−4869.
36. Gopalakrishnan, V., and Benkovic, S. (1994) *J. Mol. Biol. 269*, 4110−4115.
37. Larder, B. A. (1993) in *Cold Spring Harbor Monograph Series* (Skalka, A. M., and Goff, S. P., Eds.) pp 205−222, Cold Spring Harbor Laboratory Press, Cold Spring Harbor, NY.
38. Hostomsky, Z., Hostomska, Z., and Matthews, D. A. (1994) in *Nucleases* (Linn, S. M., Lloyd, R. S., and Roberts, R. J., Eds.) pp 341−376, Cold Spring Harbor Laboratory Press, Cold Spring Harbor, NY.
39. Hizi, A., Shaharabany, M., Tal, R., and Hughes, S. H. (1992) *J. Biol. Chem. 267*, 1293−1297.
40. Mohan, P., Loya, S., Avidan, O., Verma, S., Dhindsa, G. S., Wong, M. F., Huang, P. P., Yashiro, M., Baba, M., and Hizi, A. (1994) *J. Med. Chem. 37*, 2513−2519.

41. Loya, S., Tal, R., Kashman, Y., and Hizi, A. (1990) *Antimicrob. Agents Chemother. 34*, 2009−2012.
42. Loya, S., and Hizi, A. (1993) *J. Biol. Chem. 268*, 9323−9328.
43. Loya, S., Rudi, A., Tal, R., Kashman, Y., Loya, Y., and Hizi, A. (1994) *Arch. Biochem. Biophys. 309*, 315−322.
44. Borkow, G., Fletcher, R. S., Barnard, J., Arion, D., Motakis, D., Dmitrienko, G. I., and Parniak, M. A. (1997) *Biochemistry 36*, 3179−3185.
45. Gabbara, S., Davis, W. R., Hupe, L., Hupe, D., and Peliska, J. A. (1999) *Biochemistry 38*, 13070−13076.
46. Davis, W. R., Gabbara, S., Hupe, D., and Peliska, J. A. (1998) *Biochemistry 37*, 14213−14221.
47. Jeeninga, R. E., Huthoff, H. T., Gultyaev, A. P., and Berkhout, B. (1998) *Nucleic Acids Res. 26*, 5472−5479.
48. Guo, J., Wu, T., Bess, J., Henderson, L. E., and Levin, J. G. (1998) *J. Virol. 72*, 6716−6724.
49. Kati, W. M., Johnson, K. A., Jerva, L. F., and Anderson, K. S. (1992) *J. Biol. Chem. 267*, 25988−25997.
50. Patel, P. H., and Preston, B. D. (1994) *Proc. Natl. Acad. Sci. U.S.A. 91*, 549−553.
51. Peliska, J. A., and Benkovic, S. J. (1994) *Biochemistry 33*, 3890−3895.
52. Kulpa, D., Topping, R., and Telesnitsky, A. (1997) *EMBO J. 16*, 856−865.
53. DeStefano, J. J., Buiser, R. G., Mallaber, L. M., Bambara, R. A., and Fay, P. J. (1991) *J. Biol. Chem. 266*, 24295−24301.
54. Keck, J. L., Goedken, E. R., and Marqusee, S. (1998) *J. Biol. Chem. 273*, 34128−34133.
55. DeStefano, J. J. (1995) *Nucleic Acids Res. 23*, 3901−3908.
56. DeStefano, J. J., Mallaber, L. M., Fay, P. J., and Bambara, R. A. (1993) *Nucleic Acids Res. 21*, 4330−4338.
57. Palaniappan, C., Wisniewski, M., Jacques, P. S., Le Grice, S. F., Fay, P. J., and Bambara, R. A. (1997) *J. Biol. Chem. 272*, 11157−11164.
58. Palaniappan, C., Fuentes, G. M., Rodriguez-Rodriguez, L., Fay, P. J., and Bambara, R. A. (1996) *J. Biol. Chem. 271*, 2063−2070.
59. Katayanagi, K., Miyagawa, M., Matsushima, M., Ishikawa, M., Kanaya, S., Ikehara, M., Matsuzaki, T., and Morikawa, K. (1990) *Nature 347*, 306−309.
60. Katayanagi, K., Okumura, M., and Morikawa, K. (1993) *Proteins 17*, 337−346.
61. Yang, W., Hendrickson, W. A., Crouch, R. J., and Satow, Y. (1990) *Science 249*, 1398−1405.
62. Davies, J. d., Hostomska, Z., Hostomsky, Z., Jordan, S. R., and Matthews, D. A. (1991) *Science 252*, 88−95.
63. Johnson, M. S., McClure, M. A., Feng, D.-F., Gray, J., and Doolittle, R. F. (1986) *Proc. Natl. Acad. Sci. U.S.A. 83*, 7648−7652.
64. Kanaya, S., and Ikehara, M. (1995) *Subcell. Biochem. 24*, 377−422.
65. Telesnitsky, A., and Goff, S. P. (1993) *Proc. Natl. Acad. Sci. U.S.A. 90*, 1276−1280.
66. Sun, D., Jessen, S., Liu, C., Liu, X., Najmudin, S., and Georgiadis, M. M. (1998) *Protein Sci. 7*, 1575−1584.
67. Guo, J., Wu, W., Yuan, Z. Y., Post, K., Crouch, R. J., and Levin, J. G. (1995) *Biochemistry 34*, 5018−5029.
68. Werner, S., and Wohrl, B. M. (2000) *J. Virol. 74*, 3245−3252.

BI0015764